Rb is critical in a mammalian tissue stem cell population

Pamela L. Wenzel, Lizhao Wu, Alain de Bruin, Jean-Leon Chong, Wen-Yi Chen, Geoffrey Dureska, Emily Sites, Tony Pan, Ashish Sharma, Kun Huang, Randall Ridgway, Kishore Mosaliganti, Richard Sharp, Raghu Machiraju, Joel Saltz, Hideyuki Yamamoto, James C. Cross, Michael L. Robinson and Gustavo Leone

Genes & Dev. 2007 21: 85-97
Access the most recent version at doi:10.1101/gad.1485307

Rb is critical in a mammalian tissue stem cell population

Pamela L. Wenzel,[1,2,3,9] Lizhao Wu,[1,2,3,9] Alain de Bruin,[1,2,3,10] Jean-Leon Chong,[1,2,3] Wen-Yi Chen,[1,2,3] Geoffrey Dureska,[1,2,3] Emily Sites,[1,2,3] Tony Pan,[3,4] Ashish Sharma,[3,4] Kun Huang,[3,4] Randall Ridgway,[5] Kishore Mosaliganti,[5] Richard Sharp,[5] Raghu Machiraju,[3,4,5] Joel Saltz,[3,4] Hideyuki Yamamoto,[6] James C. Cross,[6] Michael L. Robinson,[3,7,8,11,13] and Gustavo Leone[1,2,3,12]

[1]Human Cancer Genetics Program, Department of Molecular Virology, Immunology and Medical Genetics, College of Medicine, The Ohio State University, Columbus, Ohio 43210, USA; [2]Department of Molecular Genetics, College of Biological Sciences, The Ohio State University, Columbus, Ohio 43210, USA; [3]Comprehensive Cancer Center, The Ohio State University, Columbus, Ohio 43210, USA; [4]Biomedical Informatics, Department of Pathology, College of Medicine, The Ohio State University, Columbus, Ohio 43210, USA; [5]Department of Computer Science and Engineering, The Ohio State University, Columbus, Ohio 43210, USA; [6]Department of Biochemistry and Molecular Biology, University of Calgary Faculty of Medicine, Calgary, Alberta T2N 4N1, Canada; [7]Division of Molecular and Human Genetics, Children's Research Institute, Columbus, Ohio 43205, USA; [8]Department of Pediatrics, The Ohio State University, Columbus, Ohio 43210, USA

The inactivation of the *retinoblastoma* (*Rb*) tumor suppressor gene in mice results in ectopic proliferation, apoptosis, and impaired differentiation in extraembryonic, neural, and erythroid lineages, culminating in fetal death by embryonic day 15.5 (E15.5). Here we show that the specific loss of *Rb* in trophoblast stem (TS) cells, but not in trophoblast derivatives, leads to an overexpansion of trophoblasts, a disruption of placental architecture, and fetal death by E15.5. Despite profound placental abnormalities, fetal tissues appeared remarkably normal, suggesting that the full manifestation of fetal phenotypes requires the loss of *Rb* in both extraembryonic and fetal tissues. Loss of *Rb* resulted in an increase of *E2f3* expression, and the combined ablation of *Rb* and *E2f3* significantly suppressed *Rb* mutant phenotypes. This rescue appears to be cell autonomous since the inactivation of *Rb* and *E2f3* in TS cells restored placental development and extended the life of embryos to E17.5. Taken together, these results demonstrate that loss of *Rb* in TS cells is the defining event causing lethality of $Rb^{-/-}$ embryos and reveal the convergence of extraembryonic and fetal functions of Rb in neural and erythroid development. We conclude that the *Rb* pathway plays a critical role in the maintenance of a mammalian stem cell population.

[*Keywords*: Rb; development; placenta; stem cells]

Supplemental material is available at http://www.genesdev.org.

Received August 22, 2006; revised version accepted November 10, 2006.

The *retinoblastoma* (*Rb*) tumor suppressor gene was identified more than two decades ago as the gene responsible for retinoblastoma, but has since been implicated in most human cancers. In contrast to retinoblastoma patients, inheritance of one deleted copy of *Rb* in mice did not induce retinoblastoma but did increase risk of pituitary and thyroid cancers (Jacks et al. 1992; Hu et al. 1994; Maandag et al. 1994; Williams et al. 1994; Robanus-Maandag et al. 1998; Yamasaki et al. 1998). Deletion of both copies of *Rb* in mice resulted in a broad range of severe abnormalities that lead to lethality by embryonic day 15.5 (E15.5) (Clarke et al. 1992; Jacks et al. 1992; Lee et al. 1992; Wu et al. 2003). Because *Rb* is normally expressed in all tissues of the mouse embryo, it was assumed that these developmental abnormalities were due to the absence of Rb protein in the tissues affected. Subsequent analysis of chimeric embryos suggested that Rb function is likely to be much more complex than initially suspected (Maandag et al. 1994; Lipinski et al. 2001). Indeed, recent findings showed that *Rb*-deficient embryos supplied with a wild-type placenta could develop to term and suggested a critical function of *Rb* in the placenta that might underlie many of the fetal developmental abnormalities observed in $Rb^{-/-}$ embryos (de Bruin et al. 2003; Wu et al. 2003).

Because Rb is involved in so many important pro-

[9]These authors contributed equally to this work.
Present addresses: [10]Department of Pathobiology, Faculty of Veterinary Medicine, University Utrecht, Utrecht 3584 CL, The Netherlands; [11]Zoology Department, Miami University, Oxford, Ohio 45056, USA.
Corresponding authors.
[12]E-MAIL Gustavo.Leone@osumc.edu; FAX (614) 292-3312.
[13]E-MAIL Robinsm5@muohio.edu; FAX (513) 529-6900.
Article is online at http://www.genesdev.org/cgi/doi/10.1101/gad.1485307.

cesses that are critical for embryonic development and cancer prevention there has been an intense effort to understand its biochemical functions. As a result, >110 factors have been found to bind the Rb protein, either directly or through association in a complex. Approximately two-thirds of these interacting proteins play a role in the regulation of transcription (Morris and Dyson 2001). Id2 and E2F transcription factors are among those that have emerged as relevant effectors of Rb function in vivo. For example, loss of *Id2* can rescue the viability of $Rb^{-/-}$ embryos (Lasorella et al. 2000), at least in part, by restoring normal fetal liver macrophage differentiation and erythrocyte maturation (Iavarone et al. 2004). The loss of *E2f1* or *E2f3* suppresses ectopic proliferation and apoptosis in a number of *Rb*-null tissues, and extends the life of $Rb^{-/-}$ embryos to late gestation (Tsai et al. 1998; Ziebold et al. 2001; Saavedra et al. 2002). The mechanism by which Id2, E2Fs, and other effectors of Rb act remains hotly contested, as there is evidence to support that some functions of Rb are cell autonomous and others are non-cell autonomous (Symonds et al. 1994; Lipinski et al. 2001; MacPherson et al. 2003; Iavarone et al. 2004). A prerequisite to understanding the biochemical properties of Rb that are critical for its role in development and in cancer is to identify the cell(s) where Rb is required. Understanding the dynamic interactions of Rb with its effectors might then elucidate how Rb function in this cell(s) impacts the rest of the organism.

Mutations in *Rb* but not in the related *p107* and *p130* genes are found in many types of human cancers (Weinberg 1995). While Rb and the related p107 and p130 pocket proteins can functionally compensate for one another in a number of biological settings, they also appear to regulate some processes uniquely (Lee et al. 1996; Mulligan and Jacks 1998; Lipinski and Jacks 1999; Vanderluit et al. 2004). $Rb^{-/-}$ mice die during gestation with anemia, placental defects, and widespread hyperproliferation and apoptosis, whereas $p130^{-/-}$ and $p107^{-/-}$ mice can develop normally (Cobrinik et al. 1996; Lee et al. 1996; LeCouter et al. 1998a,b; Mulligan and Jacks 1998). These distinct phenotypes, however, may reflect spatial differences in their expression pattern. The only clear biochemical distinctions between the related pocket proteins are their E2F-binding preferences in vitro. Whereas E2F4 and E2F5 can associate with all pocket proteins, E2F1, E2F2, and E2F3 normally bind exclusively to Rb (Ewen et al. 1992; Faha et al. 1992; Lees et al. 1992; Li et al. 1993; Lipinski and Jacks 1999). Despite all we have learned about this family of proteins, the functions that endow Rb with tumor suppressor activity have yet to be defined. The tumor suppressor function that distinguishes Rb from the other pocket proteins might be related to the unique function Rb plays during development. This uniqueness may originate from the biochemical properties of Rb or the nature of the cell in which Rb functions.

As in cancer and other complex-trait diseases, the developmental abnormalities caused by the inactivation of *Rb* are likely based on multiple interactions within and between different cell types and organs. Here, we designed digital algorithm-based three-dimensional (3D) image analysis systems and lineage-specific *cre* mice to dissect the spatial and temporal requirement of *Rb* gene networks within the developing embryo. We show that Rb is required in trophoblast stem (TS) cells but not in trophoblast derivatives of the placenta. The unique requirement for Rb in the TS cell population, and not in its derivatives, points to a stem cell-specific function of *Rb* not shared by the related p107 and p130 family members. Further, we find that a critical role for Rb in this TS cell compartment is mediated by one of its binding partners, E2F3.

Results

3D image analysis reveals global disruption of Rb mutant placentas

The global impact of *Rb* loss on the placenta was visualized by a digital 3D imaging system. The 3D renderings of the entire placenta presented in Figure 1 illustrate the cellular complexity of the maternal-derived decidual layer and two of the major extraembryonic cell derivatives: labyrinth trophoblasts and spongiotrophoblasts. The placenta vasculature embedded within the extraembryonic layer provides the main site of nutrient–waste exchange between the mother and fetus via a network of maternal sinusoids juxtaposed to fetal blood vessels. A comparison between littermates revealed a significant decrease of vascular space in *Rb* mutant placentas, consistent with their impaired transport function (Fig. 1B; Wu et al. 2003). This vascular defect was compounded by a concomitant decrease in the total volume of the labyrinth. In addition, complementary morphometric analyses indicated a dramatic perturbation of the mutant labyrinth–spongiotrophoblast interface. These measurements revealed the presence of shallow finger-like spongiotrophoblast projections that fail to properly invade the mutant labyrinth layer, highlighting the chaotic organization within this region of *Rb* mutant placentas (Fig. 1A [two bottom panels], B). Indeed, necrosis, clustering, and multinucleation of *Rb*-deficient trophoblasts were especially acute near the labyrinth–spongiotrophoblast interface. These observations illustrate the global disruption of labyrinth and vascular architecture that results from the hyperproliferation of $Rb^{-/-}$ trophoblasts (see Fig. 4A, below) and suggest that placental dysfunction could stem from a defect in one or more of the extraembryonic cell lineages.

Fetuses supplied with an Rb mutant placenta are embryonic lethal

Previous embryo aggregation studies have shown that $Rb^{+/+}$–$Rb^{-/-}$ chimeric fetuses, as well as $Rb^{-/-}$ fetuses, can survive to birth when supplied with a wild-type placenta (Maandag et al. 1994; Williams et al. 1994; Wu et al. 2003). To examine the requirement of *Rb* in extraembryonic lineages we used morula–embryonic stem (ES) cell aggregation techniques to generate chimeric fetuses that had *Rb*-deficient placentas (Wang et al. 1997). $Rb^{+/+}$

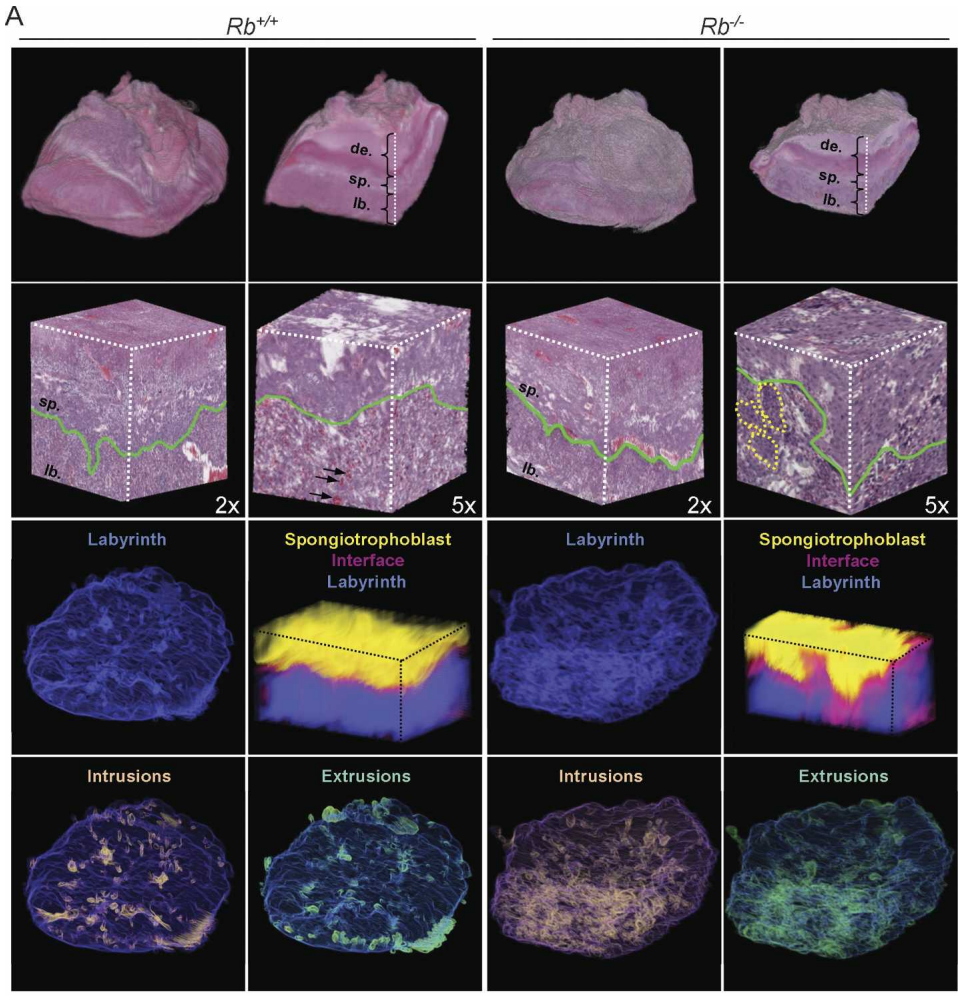

B

Morphometric analysis of *Rb* mutant placentas

	$Rb^{+/+}$	$Rb^{-/-}$
Labyrinth Volume (mm^3)	11 9	7.9[a] 8.2[a]
Percent Vascular Space	31.9 20.2	22[b] 12[b]
Labyrinth-Spongio. Interface (pixels)	1738 2374	3413[c] 4210[c]
Labyrinth-Spongio. Intrusions (pixels)[d]	16.5 ± 6.3 14.5 ± 5.5	20.5 ± 11.1 17.1 ± 7.5
Labyrinth-Spongio. Extrusions (pixels)[d]	10.5 ± 5.9 8.1 ± 3.7	12.9 ± 9.7 11.3 ± 7.2

[a] Two-tailed paired t-test $p<0.02$; [b] two-tailed paired t-test $p<0.0001$; [c] one-tailed paired t-test $p<0.05$. Comparisons were performed between $Rb^{+/+}$ and $Rb^{-/-}$. [d] Lower mean values indicate fewer finger-like spongiotrophoblast projections, and lower standard deviations indicate that projections are uniformly distributed.

Figure 1. Three-dimensional image analysis reveals global disruption of *Rb* mutant placentas. (*A*, panels in *first row*) Representative 3D images derived from H&E-stained sections of whole placentas that were scanned, registered, and stitched together. A representative internal slice reveals the major cell layers of the placenta. (de) Decidua; (sp) spongiotrophoblast; (lb) labyrinth trophoblast. (Panels in *second row*) Higher-magnification (2× and 5×) cubic images of the labyrinth–spongiotrophoblast interface. Green lines represent the boundary between the labyrinth–spongiotrophoblast interface; dotted yellow lines encircle clusters of $Rb^{-/-}$ trophoblasts that are embedded within the labyrinth; arrows point to typical blood spaces visible in the $Rb^{+/+}$ placenta. (Panels in *third row*) Volumetric rendering of the labyrinth layer (blue). Morphometric analysis of the labyrinth (blue) and spongiotrophoblast (yellow) layers are depicted by cubic images at high resolution. The magenta area represents the region of contact between the labyrinth and spongiotrophoblast layers; note the expanded interface zone between these two layers in the $Rb^{-/-}$ placenta. (Panels in *fourth row*) Morphometric analyses of spongiotrophoblast intrusions and extrusions into the labyrinth layer (blue) are visually rendered in orange and green, respectively. The genotypes of each placenta are indicated at the *top* ($Rb^{+/+}$, $n = 3$; $Rb^{-/-}$, $n = 3$). For a rotational view of whole placentas and magnified cubic images, see also http://tinyurl.com/bc6ka. (*B*) Morphometric analysis of *Rb* mutant placentas.

and $Rb^{-/\Delta 19}$ E2.5 diploid morula were aggregated with wild-type YC5 ES cells expressing the yellow fluorescent protein (YFP) (Hadjantonakis et al. 2002); the use of two different *Rb*-null alleles (Rb^{-} and $Rb^{\Delta 19}$) facilitated the genotyping of the aggregated embryos (Jacks et al. 1992; Marino et al. 2000). In this setting, diploid morula contribute to both extraembryonic and fetal lineages but ES cells contribute only to fetal lineages. Hence, the resulting placentas would be either genetically $Rb^{+/+}$ or $Rb^{-/\Delta 19}$ and fetuses would be chimeric (James et al. 1995). As evaluated by both fluorescent microscopy and Southern blot analysis, chimeric fetuses were uniformly enriched for wild-type YFP-positive cells (>95% $Rb^{+/+}$) (Fig. 2A; data not shown). As expected, embryos reconstituted with $Rb^{+/+}$ morula had normal placentas, with spongiotrophoblast finger-like projections extending into the labyrinth and trophoblasts uniformly organized around the placental vasculature (Fig. 2B). In contrast, fetuses derived from $Rb^{-/\Delta 19}$ morula had placentas with a severely disrupted labyrinth architecture typical of $Rb^{-/-}$ embryos. While most fetuses associated with wild-type placentas were alive at each of the time points examined (54/57), more than half of the fetuses associated with $Rb^{-/\Delta 19}$ placentas were dead by E13.5 (15/25), and all were dead by E15.5 (9/9) (Fig. 2C). Thus, in contrast to previous work showing that $Rb^{+/+}$-$Rb^{-/-}$ chimeric fetuses supplied with wild-type placentas can be carried to term (Maandag et al. 1994; Williams et al. 1994), our work here shows that chimeric fetuses supplied with $Rb^{-/\Delta 19}$ placentas die by E15.5. These morula–ES cell aggregation studies demonstrate that *Rb*-deficient extraembryonic lineages are functionally responsible for the global disruption of the placenta and lethality in $Rb^{-/-}$ embryos.

A

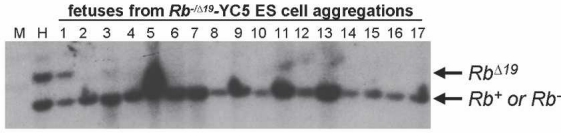

B

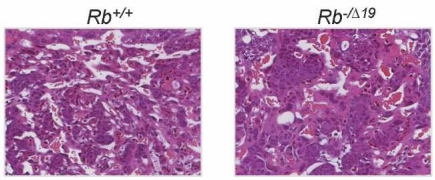

C

Genotypic analysis of aggregated diploid morula-ES cell embryos

placenta genotype	E12.5	E13.5	E15.5
$Rb^{+/+}$	9	25 (2)	21 (1)
$Rb^{+/-}$	20 (6)	62 (9)	43 (12)[a]
$Rb^{-/-}$	4 (2)	21 (13)[b]	9 (9)[b]

( ) dead embryos; Fisher exact probability test [a](p=0.0245) [b](p<0.0001) compared to $Rb^{+/+}$ embryos

Figure 2. Embryos reconstituted with $Rb^{+/+}$ and $Rb^{-/\Delta 19}$ placentas. (*A*) Southern blot analysis of aggregated chimeric fetuses hybridized with an Rb-specific probe that differentiates between the $Rb^{\Delta 19}$ and Rb^{+}/Rb^{-} alleles (indicated on the *right*). (M) Lane loaded with DNA ladder marker; (H) $Rb^{\Delta 19/+}$ control DNA sample. Note the low contribution of YC5 ES cells ($Rb^{+/+}$) to chimeric fetus number 1; all others fetuses contained >95% contribution from YC5 ES cells. (*B*) Placental sections from representative aggregated embryos with the indicated genotypes were stained with H&E. Note the clusters of small cuboidal trophoblast cells in $Rb^{-/\Delta 19}$ placentas. Original magnification, 20×. (*C*) Genotypic analysis of aggregated diploid morula–ES cell embryos.

Generation of extraembryonic lineage-specific cre mice

To define the contributions made by *Rb* in the various extraembryonic lineages we initially targeted the ablation of *Rb* in TS cells, which are thought to give rise to labyrinth trophoblasts, spongiotrophoblasts and giant trophoblasts. To this end, expression of *cre* in TS cells was driven by a transgene (*CYP19-cre*) containing a 504-base-pair (bp) fragment of the human *CYP19* promoter previously shown to promote expression of a reporter gene in the mouse placenta (Kamat 1999; Kamat et al. 2005). As determined by X-gal histochemical staining, *cre* expression could be detected in *CYP19-cre;-Rosa*$^{+/LoxP}$ TS cells cultured in vitro from E3.5 blastocyst explants (P. Wenzel, unpubl.). Moreover, analysis of *CYP19-cre;Rosa*$^{+/LoxP}$ reporter embryos confirmed expression of *cre* in the ectoplacental cone and extraembryonic ectoderm where TS cells reside at E6.5 and E8.5 (Fig. 3A; Tanaka et al. 1998; Uy et al. 2002). By the time TS cells give rise to the mature trilaminate cell layers of the placenta, which occurs at around E10.5–E13.5, *cre* expression could be visualized throughout the labyrinth and spongiotrophoblast of the placenta but not in the primitive endoderm and ectoderm derivatives that populate the yolk sac (Fig. 3A). In situ hybridization with a spongiotrophoblast-specific probe (*Tpbp*) confirmed the expression of *cre* in these cells and its absence in many of the adjacent giant cells (Fig. 3B). This latter unexpected observation suggests that *cre* expression in TS cells is either incomplete, turned on after giant cell fate determination, or restricted to a TS cell subpopulation lacking the ability to differentiate into all giant cell types. Some fetal tissues also expressed *cre*, but these were primarily restricted to localized areas in the skin and occasional lens cells of the eye (Fig. 3A; Supplementary Fig. S1A; P. Wenzel, unpubl.).

Specific loss of Rb in extraembryonic TS cells causes death by E15.5

To evaluate the developmental impact of ablating *Rb* specifically in TS cells we analyzed the offspring from *CYP19*-cre;$Rb^{-/+}$ and $Rb^{LoxP/LoxP}$;$Rosa^{LoxP/LoxP}$ intercrosses. In contrast to $Rb^{-/LoxP}$;$Rosa^{+/LoxP}$ embryos, placentas associated with E13.5 *CYP19-cre*;$Rb^{-/LoxP}$;$Rosa^{+/LoxP}$ embryos had a severe disruption of labyrinth architecture that was characterized by clustering of trophoblasts, a marked reduction in maternal–fetal blood

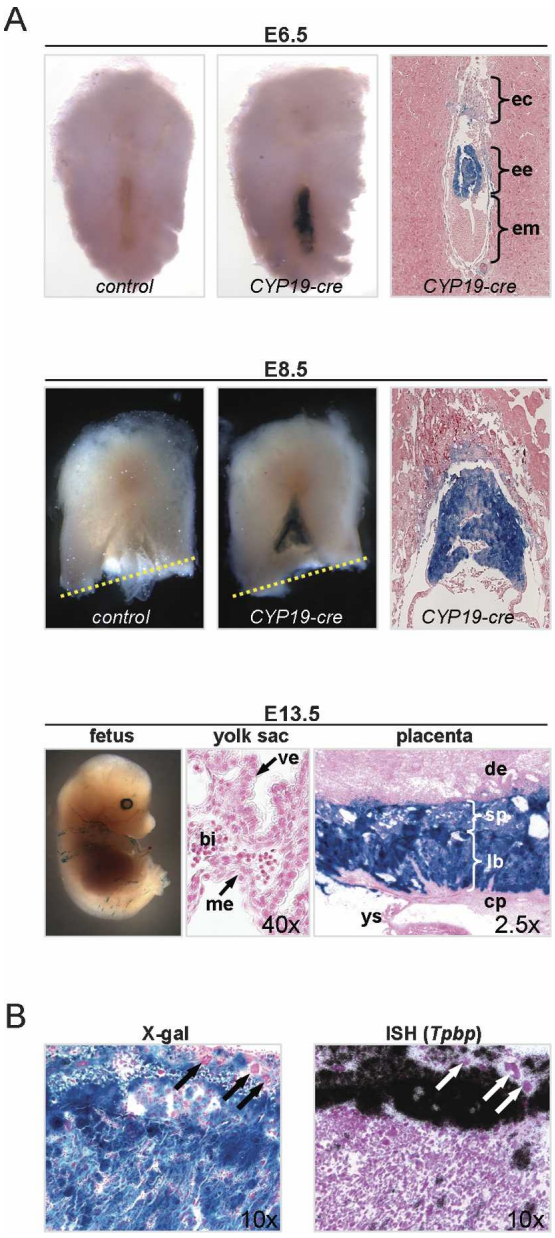

Figure 3. The *CYP19-cre* transgene drives expression of *cre* in TS cell lineages. (*A*) *CYP19-cre* transgenic mice were crossed to $Rosa^{LoxP/LoxP}$ reporter mice and analyzed for β-galactosidase activity to establish the pattern and timing of *cre* expression in the E6.5 and E8.5 embryo (counterstained with eosin) and E13.5 (counterstained with nuclear fast red) fetus, yolk sac, and placenta. The dotted yellow line shows the incision site made for removal of the fetus for genotyping; note that the fetus is not shown for the E8.5 panels. (ec) Ectoplacental cone; (ee) extraembryonic ectoderm; (em) embryonic endoderm; (me) extraembryonic mesoderm; (ve) visceral endoderm; (bi) blood island; (de) decidua; (sp) spongiotrophoblast; (lb) labyrinth trophoblast; (cp) chorionic plate; (ys) yolk sac. (*B*, *right*) Placenta sections from E13.5 embryos were hybridized with a spongiotrophoblast-specific (*Tpbp*) RNA probe and were counterstained with hematoxylin. Micrographs of sections hybridized with a sense RNA *Tpbp* probe are not shown. (*Left*) An adjacent section was stained by X-gal and counterstained with nuclear fast red. Giant trophoblasts that did not express *cre* are indicated by arrows.

spaces, and occasional necrosis of trophoblasts near the labyrinth–spongiotrophoblast interface (Fig. 4A, left panels). BrdU-specific immunofluorescence assays confirmed an increase in the proliferation of trophoblasts that had the morphological features of TS cells and that we previously showed to express *Eomes* (Figs. 4A, 7B [below]; Wu et al. 2003). Whereas $Rb^{-/LoxP}$;$Rosa^{+/LoxP}$ offspring, which were alive at all stages of development, some *CYP19-cre*;$Rb^{-/LoxP}$;$Rosa^{+/LoxP}$ embryos were dead as early as E11.5 (2/9), approximately one-quarter were dead by E13.5 (11/49), two-thirds were dead by E15.5 (7/11), and all embryos were dead by E17.5 (5/5) (Fig. 4B). This range in the timing of lethality is similar to that previously found for $Rb^{-/-}$ embryos (Fig. 4B; Clarke et al. 1992; Jacks et al. 1992; Lee et al. 1992).

The early lethality of *Rb* mutant embryos could stem from the restricted pattern of pocket protein expression in TS cells or from a unique function of Rb in these cells that is not shared by p107 or p130. The Western blot and real-time RT–PCR analysis in Figure 4, C and D, show that p107 and p130 are indeed expressed in cultured $Rb^{+/+}$ TS cells. As has been shown in other cell types (Classon et al. 2000), the loss of *Rb* in TS cells led to the compensatory up-regulation of p130 and, to a lesser extent, p107 (Fig. 4C,D). Despite the increase in p107 and p130 expression, $Rb^{-/-}$ TS cells had a higher index of proliferation as determined by BrdU incorporation and histone H3 phosphorylation (Fig. 4E). Consistent with these findings, pocket protein function in trophoblasts appears to be conferred by Rb alone, since loss of *Rb* and not *p107* or *p130* causes the severe placental defects described in this study (P. Wenzel, unpubl.). Together, these data suggest that Rb is endowed with a singular role in the control of TS cell proliferation and placental development.

Analysis of some embryos derived from a second *CYP19-cre* founder line revealed that *cre* failed to be expressed in TS cells, but was instead expressed in labyrinth trophoblast and visceral endoderm lineages (*CYP19lab-cre*) (Fig. 5A,C). We also generated transgenic mice that expressed *cre* specifically in spongiotrophoblasts by linking the *cre* ORF to a 1.1-kb fragment of the mouse *Tpbp* promoter known to drive expression in this cell lineage (Calzonetti et al. 1995) (*Tpbp-cre*) (Fig. 5B,D; A.L. Fortier, H. Yamamoto, and J.C. Cross, in prep.). By similar breeding strategies as described above, we obtained offspring from crosses between *CYP19lab-cre*;$Rb^{-/+}$ and $Rb^{LoxP/LoxP}$;$Rosa^{LoxP/LoxP}$ mice as well as from *Tpbp-cre*;$Rb^{-/+}$ and $Rb^{LoxP/LoxP}$;$Rosa^{LoxP/LoxP}$ mice. Interestingly, we found that the targeted inactivation of *Rb* from either of these two TS cell derivatives had no adverse effect on placental development and the associated fetuses could be carried to term normally (Fig. 5E–H; data not shown). These results suggest that the critical function of *Rb* resides in TS cells prior to their commitment to labyrinth trophoblast and spongiotrophoblast cell fates. Together, the embryo aggregation and trophoblast-specific conditional deletion approaches define loss of *Rb* in TS cells as the critical event causing lethality of $Rb^{-/-}$ embryos.

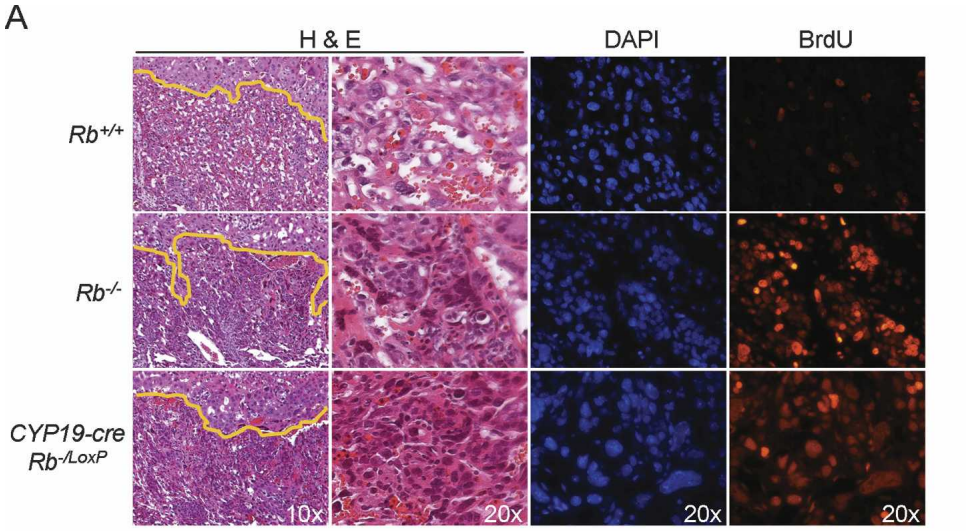

B

Genotypic analysis of embryos

Rb$^{+/-}$ x *Rb*$^{+/-}$	E11.5	E13.5	E15.5	E17.5
Rb$^{+/+}$	-	211 (2)	37 (1)	4
Rb$^{+/-}$	-	396 (3)	52 (1)	24
Rb$^{-/-}$	-	141 (34)[a]	21 (17)[a]	5 (5)[b]
CYP19-cre;Rb$^{+/-}$ x *Rb*$^{LoxP/LoxP}$;*Rosa*$^{LoxP/LoxP}$	E11.5	E13.5	E15.5	E17.5
Rb$^{+/LoxP}$	2	42	6	12
Rb$^{-/LoxP}$	3	49 (1)	7	17
Cre Rb$^{+/LoxP}$*Rosa*$^{+/LoxP}$	5	49 (2)	12	12
Cre Rb$^{-/LoxP}$*Rosa*$^{+/LoxP}$	9 (2)	49 (11)[b]	11 (7)[c]	5 (5)[b]

() number of dead embryos; Chi-square test for association [a](p<0.0001), Fisher exact probability test
[b](p<0.01), [c](p<0.05) compared to *wild type*.

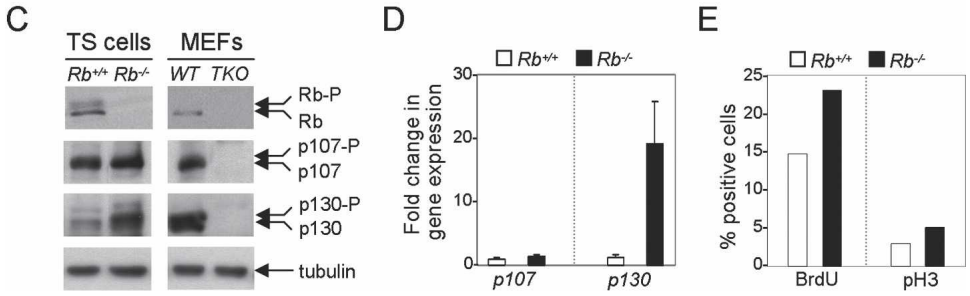

Figure 4. Rb ablation in the placenta causes lethality and disruption of labyrinth architecture. (*A*) Sections of placentas were stained with H&E (two *left* panels) or processed for immunofluorescence using BrdU-specific antibodies and counterstained with DAPI (two *right* panels). Yellow lines indicate the boundary between the labyrinth and spongiotrophoblast cell layers. The original magnification is indicated within the *bottom* panels for each column. (*B*) Genotypic analysis of embryos. (*C*) Pocket proteins were detected by Western blot in TS cells and mouse embryonic fibroblasts (MEFs). TKO is a cell line triply deleted for Rb, p107, and p130. (*D*) Expression of *p107* and *p130* in *Rb*$^{+/+}$ and *Rb*$^{-/-}$ TS cells was measured by real-time RT–PCR using primers listed in Supplementary Figure S3. (*E*) Immunofluorescence of BrdU incorporation and phosphorylation of histone H3 was used as an indicator of DNA synthesis and mitosis, respectively, in cultured TS cells.

E2F3 is a key mediator of Rb function in TS cells

Having identified the critical cell where many *Rb*$^{-/-}$ placental and fetal defects originate, we wondered if key effectors of Rb might also function in TS cells to dictate placental and fetal developmental programs. Among the many proteins that physically interact with Rb, the E2F transcription factors have emerged as critical Rb-binding partners. E2Fs consist of several family members thought to be functionally redundant that regulate simi-

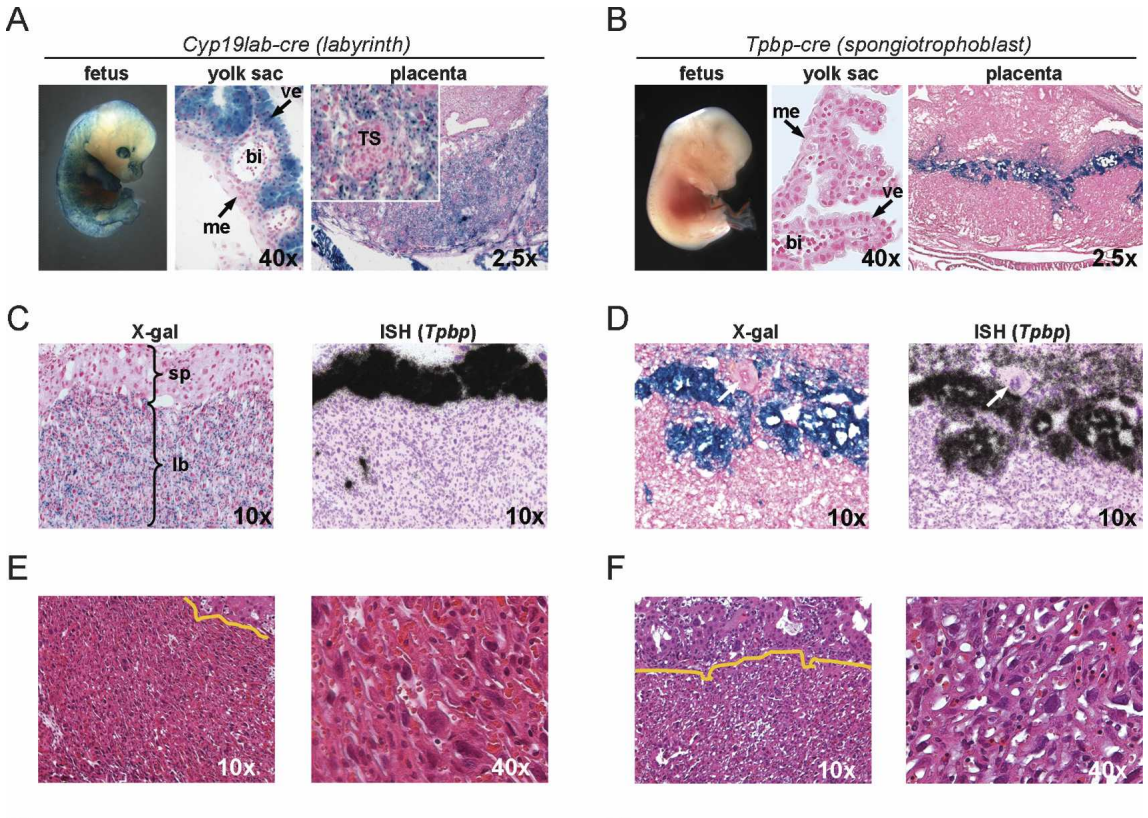

G

Genotypic analysis of *CYP19-cre;Rb$^{-/LoxP}$* embryos

Cyp19lab-cre (labyrinth)	E17.5
Cre Rb$^{+/LoxP}$Rosa$^{+/LoxP}$	4
Cre Rb$^{-/LoxP}$Rosa$^{+/LoxP}$	2

H

Genotypic analysis of *Tpbp-cre;Rb$^{-/LoxP}$* embryos

Tpbp-cre	E13.5	Newborn
Rb$^{+/LoxP}$Rosa$^{+/LoxP}$	2	16
Rb$^{-/LoxP}$Rosa$^{+/LoxP}$	6	19
Cre Rb$^{+/LoxP}$Rosa$^{+/LoxP}$	11	16
Cre Rb$^{-/LoxP}$Rosa$^{+/LoxP}$	2	12

Figure 5. Deletion of *Rb* in labyrinth trophoblasts or spongiotrophoblasts does not affect embryonic development. (*A*,*B*) Whole mount of the fetus and sections of the yolk sac and placenta from *CYP19lab-cre;Rosa$^{+/LoxP}$* (*A*) and *Tpbp-cre;Rb$^{-/LoxP}$;Rosa$^{+/LoxP}$* (*B*) embryos were stained with X-gal and counterstained with nuclear fast red. *Inset* represents a higher-magnification micrograph of a representative TS cell cluster, which does not stain positively with X-gal. (me) Extraembryonic mesoderm; (ve) visceral endoderm; (bi) blood island; (TS) cluster of cells with TS cell morphology. (*C*,*D*) In situ hybridization of placenta sections from E13.5 *CYP19lab-cre;Rb$^{-/LoxP}$;Rosa$^{+/LoxP}$* (*C*) or E13.5 *Tpbp-cre;Rb$^{-/LoxP}$;Rosa$^{+/LoxP}$* (*D*) embryos using an antisense RNA *Tpbp* probe. Micrographs of sections hybridized with a sense RNA *Tpbp* probe are not shown. Adjacent sections were stained with X-gal as indicated. Arrows point to a giant trophoblast. (sp) Spongiotrophoblast; (lb) labyrinth trophoblast. (*E*,*F*) Sections of E17.5 *CYP19lab-cre Rb$^{-/LoxP}$;Rosa$^{+/LoxP}$* placentas (*E*) and E13.5 *Tpbp-cre;Rb$^{-/LoxP}$;Rosa$^{+/LoxP}$* placentas (*F*) stained with H&E. (*G*,*H*) Genotypic analyses of embryos derived from *CYP19lab-cre;Rb$^{+/-}$* and *Rb$^{LoxP/LoxP}$;Rosa$^{LoxP/LoxP}$* intercrosses (*G*), as well as from *Tpbp-cre;Rb$^{+/-}$* and *Rb$^{LoxP/LoxP}$;Rosa$^{LoxP/LoxP}$* intercrosses (*H*).

lar sets of target genes; however, some studies suggest that there are at least two distinct classes of E2Fs: activators and repressors (Trimarchi and Lees 2001).

To address the potential role of E2F family members in mediating *Rb* mutant phenotypes we initially measured their expression in *Rb* mutant placentas. As determined by real-time RT–PCR assays, *E2f1* and *E2f3a* expression was up-regulated two- to threefold in *Rb*-deficient placentas, whereas *E2f2*, *E2f3b*, *E2f4*, *E2f5*, *E2f6*, *E2f7*, and *E2f8* expression remained relatively unchanged (Fig. 6A). We then analyzed the consequence resulting from the deletion of each family member in an *Rb* mutant context. Histological evaluation of Rb–E2F doubly deficient embryos revealed that loss of *E2f3*, but not *E2f1*, *E2f2*, *E2f4*, and *E2f5*, significantly suppressed the widespread overproliferation and clumping of abnormal multinucleated trophoblasts typically observed in *Rb*-deficient placentas. While a few *Rb–E2f1* doubly deficient placentas had a milder *Rb* mutant placenta phenotype (data not shown), the majority of embryos collected at ages later than E13.5 were not alive (Fig. 6C). Deletion of *E2f3* was able to abrogate the *Rb$^{-/-}$* phenotype to the extent that all double-knockout embryos at E15.5 were alive (Fig. 6B,C), an age when ~80% of *Rb*-deficient embryos are

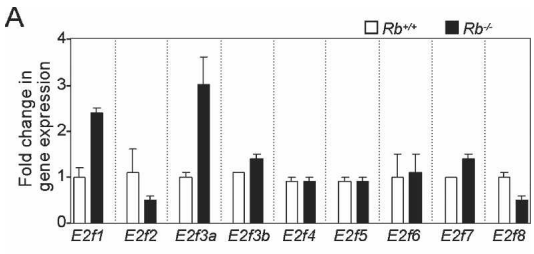

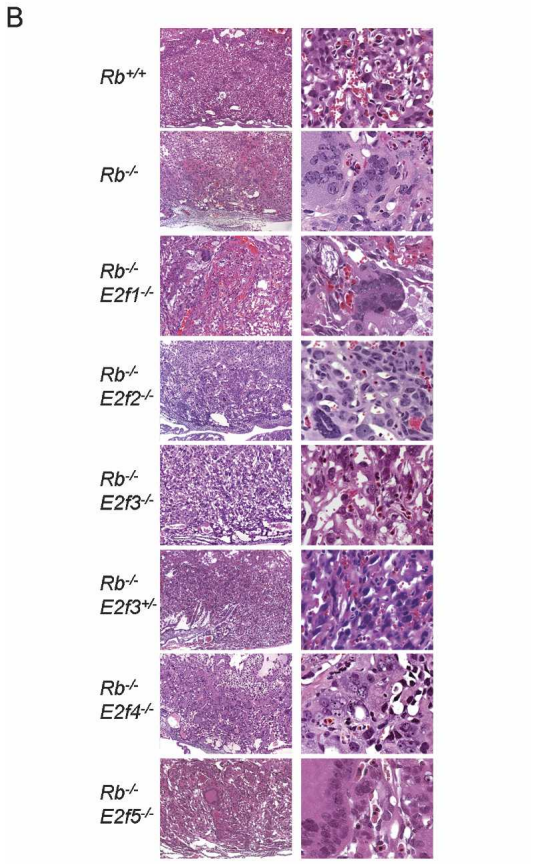

C

Genotypic analysis of *Rb–E2f* double mutant embryos

	E12.5	E13.5	E15.5
Rb$^{-/-}$ *E2f1*$^{-/-}$	–	8 (3) [15]	9 (5) [11]
Rb$^{-/-}$ *E2f2*$^{-/-}$	–	14 (3) [16]	3 (3) [4]
Rb$^{-/-}$ *E2f3*$^{-/-}$	–	19 (0) [9]	9 (0) [6]
Rb$^{-/-}$ *E2f4*$^{-/-}$	3 (1) [3]	2 (1) [6]	–
Rb$^{-/-}$ *E2f5*$^{-/-}$	5 (1) [4]	8 (3) [8]	9 (7) [15]

(dead mice) [expected mice]

Figure 6. Loss of *E2f3* in *Rb*-null TS cells suppresses mutant phenotypes. (*A*) Expression of *E2f1–8* in *Rb*$^{+/+}$ and *Rb*$^{-/-}$ placentas was measured by real-time RT–PCR assays using primers described in Supplementary Figure S3. (*B*) Placental sections from embryos with the indicated genotypes were stained with H&E. Note that loss of *E2f3* suppressed the formation of large clumps of dysplastic trophoblasts. (*C*) Genotypic analysis of double-knockout embryos derived from crosses between *Rb*$^{+/-}$ and either *E2f*$^{+/-}$ or *E2f*$^{-/-}$ mice.

found dead (Fig. 4B). Loss of even one allele of *E2f3* resulted in a partial rescue of the *Rb*$^{-/-}$ placental defect, with some variability observed between the embryos analyzed (Fig. 6B; data not shown).

To directly test whether *Rb*$^{-/-}$ placental defects are a result of deregulated E2F3 activity in TS cells, we interbred *CYP19-cre;Rb*$^{-/+}$*;E2f3*$^{LoxP/LoxP}$ and *Rb*$^{LoxP/LoxP}$*; E2f3*$^{LoxP/LoxP}$*;Rosa*$^{LoxP/LoxP}$ mice and analyzed the resulting embryos. Placentas with *Rb–E2f3*-deficient TS cells had a relatively normal spongy architecture with little evidence of hyperproliferative trophoblasts (Fig. 7A,B). While some regional clumping could still be observed in these doubly deficient placentas, the presence of large dysplastic trophoblasts and the high degree of necrosis typically observed in *Rb* mutant placentas was

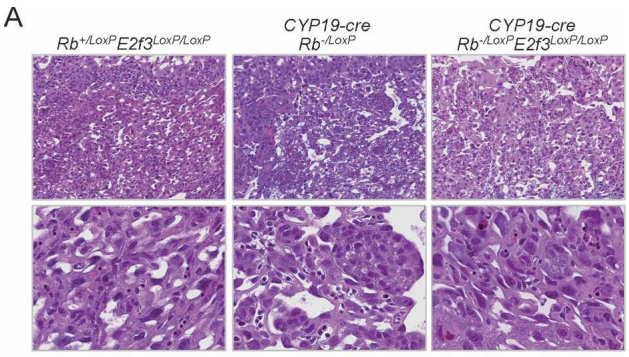

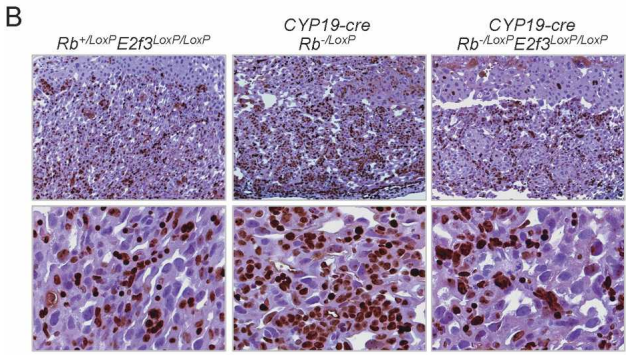

C

Genotypic analysis of *Rb-E2f3* mutant embryos

CYP19-cre;Rb$^{+/-}$*;E2f3*$^{LoxP/LoxP}$ x *Rb*$^{LoxP/LoxP}$*;E2f3*$^{LoxP/LoxP}$*;Rosa*$^{LoxP/LoxP}$	E13.5	E16.5	E17.5
Rb$^{+/LoxP}$ *E2f3*$^{LoxP/LoxP}$*Rosa*$^{+/LoxP}$	9	5	6
Rb$^{-/LoxP}$ *E2f3*$^{LoxP/LoxP}$*Rosa*$^{+/LoxP}$	12	8	8 (1)
Cre Rb$^{+/LoxP}$*E2f3*$^{LoxP/LoxP}$*Rosa*$^{+/LoxP}$	5 (1)	4	3
Cre Rb$^{-/LoxP}$*E2f3*$^{LoxP/LoxP}$*Rosa*$^{+/LoxP}$	4	3	7 (5)[a]

() number of dead embryos; Fisher exact probability test [a](p=0.016) compared to *wild type*.

Figure 7. Conditional deletion of *Rb* and *E2f3* in TS cells. (*A*) Placental tissue sections with the indicated genotypes were stained with H&E and micrographed at low (*top* panels) and high (*bottom* panels) magnification. (*B*) Similar sections as in *A* were processed for immunohistochemistry using Ki67-specific antibodies and counterstained with hematoxylin; *top* and *bottom* panels show micrographs at low and high magnification, respectively. (*C*) Genotypic analysis of embryos derived from crosses between *CYP19-cre;Rb*$^{-/LoxP}$*;E2f3*$^{LoxP/LoxP}$*;Rosa*$^{+/LoxP}$ and *Rb*$^{-/LoxP}$*;E2f3*$^{LoxP/LoxP}$*;Rosa*$^{+/LoxP}$ mice.

significantly diminished. In contrast to embryos associated with placentas having *Rb*-deficient TS cells, which died by E15.5 (Fig. 4B), embryos with doubly deficient TS cells were still alive as late as E17.5 (Fig. 7C). These results phenocopy those obtained in $Rb^{-/-}E2f3^{-/-}$ embryos and suggest a cell-autonomous role for *E2f3* in TS cells that is responsible for the lethality of *Rb*-deficient embryos by E15.5. The fact that placentas derived from double-mutant TS cells cannot carry fetuses all the way to term, however, suggests that some functions of Rb in the placenta are independent of its interaction with E2F3 and the control of proliferation, but presumably are related to the control of trophoblast differentiation.

Loss of Rb in TS cells leads to ectopic apoptosis and erythroid defects in the fetus

Previous work suggested that *Rb* function in the placenta dictates critical developmental events in the fetus, including the control of apoptosis in the CNS and of erythropoiesis in fetal livers (de Bruin et al. 2003; Wu et al. 2003). We therefore examined the developmental consequences stemming from the ablation of *Rb* in TS cells. As expected, $CYP19\text{-}cre;Rb^{-/LoxP};Rosa^{+/LoxP}$ E13.5 fetuses had normal numbers of proliferating cells in the CNS, peripheral nervous system (PNS), lens, liver, and skeletal muscle (Supplementary Fig. S1A,B; data not shown). However, there was clear evidence of ectopic apoptosis in areas of the brainstem surrounding the fourth ventricle. The severity of this defect, though, was considerably less pronounced than in $Rb^{-/-}$ embryos (Fig. 8A,B). Other compartments of the brain, such as the cerebellum and midbrain, and tissues of the PNS, lens, liver, and skeletal muscle did not exhibit any signs of increased cell death (Fig. 8B; Supplementary Fig. S1A; data not shown).

Impaired red blood cell (RBC) differentiation leading to anemia is another hallmark phenotype of *Rb* knockout mice. While $CYP19\text{-}cre;Rb^{-/LoxP};Rosa^{+/LoxP}$ fetuses had normal coloration and appearance, they had a small but significant increase in immature nucleated RBCs (Fig. 8A,B). Erythropoietic defects in *Rb* mutant embryos can be mediated, at least in part, through non-cell-autonomous mechanisms involving liver-specific macrophages

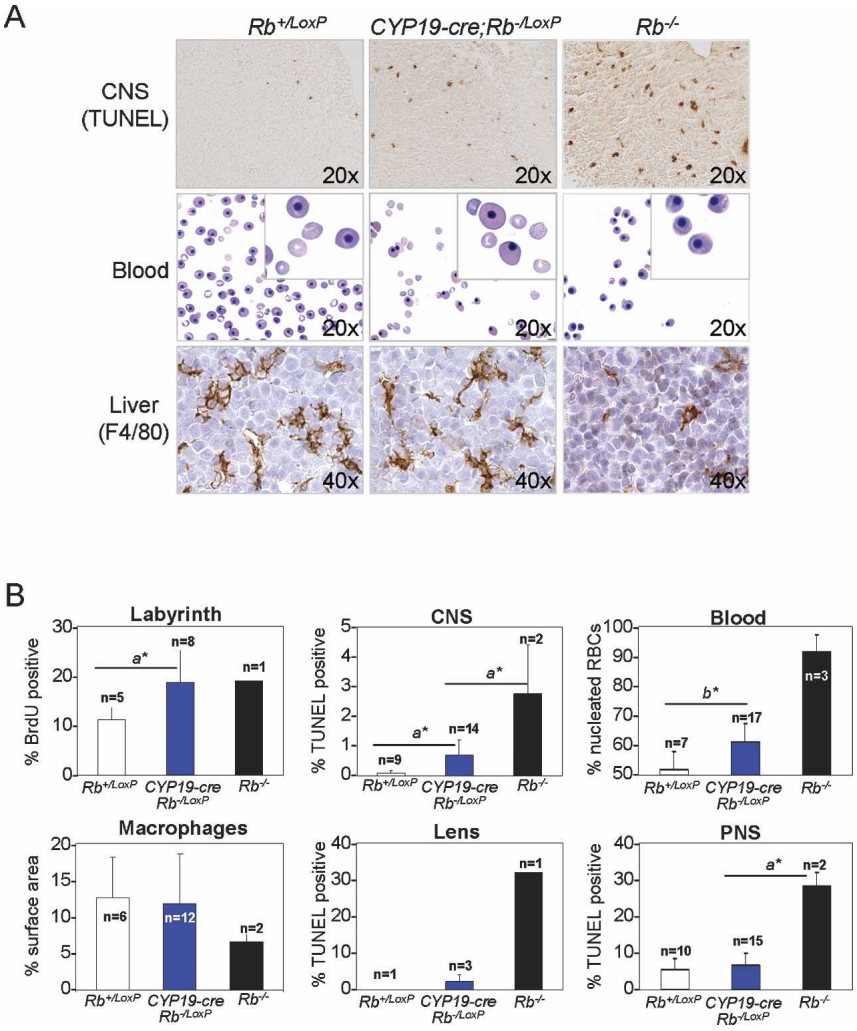

Figure 8. Loss of *Rb* in TS cells partially disrupts fetal development. (*A*) Analysis of E13.5 fetal tissues from $CYP19\text{-}cre;Rb^{-/LoxP};Rosa^{+/LoxP}$ and control embryos. Apoptosis was measured in the CNS by TUNEL assays, erythrocyte maturation in peripheral blood smears was monitored by staining with Giemsa, and the presence of macrophages in the liver was assessed by immunostaining with F4/80-specific antibodies and counterstaining with hematoxylin. Original magnifications are indicated for each panel and *insets* were 40×. (*B*) Quantification of proliferation and apoptosis of the indicated tissues as determined by BrdU- and TUNEL-assays, respectively. Note the presence of a small percentage of TUNEL-positive lens fiber cells present in $CYP19\text{-}cre;Rb^{-/LoxP};Rosa^{+/LoxP}$ embryos that arises as a consequence of occasional *cre*-expressing cells in the lens driven by this transgene. Hematopoietic differentiation was measured by the percentage of nucleated RBCs in peripheral blood (Blood) and by the amount of macrophages (% surface area) present in fetal livers (Macrophages). (a*) Mann-Whitney U-test, $p < 0.05$; (b*) Wilcoxon Signed Rank test, $p = 0.002$.

(Wu et al. 2003; Iavarone et al. 2004). Thus, we analyzed *CYP19-cre;Rb*$^{-/LoxP}$*;Rosa*$^{+/LoxP}$ fetal livers but found no significant change in F4/80-positive macrophages (Fig. 8A,B). These results suggest a macrophage-independent role of the placenta in RBC differentiation. Parallel analysis of chimeric embryos with *Rb* mutant placentas generated by tetraploid and diploid aggregation techniques yielded results identical to those obtained by the genetic ablation of *Rb* in TS cells (Supplementary Fig. S2; data not shown). These results demonstrate that *Rb* deficiency in TS cells causes some ectopic apoptosis and impaired RBC differentiation but that this non-cell-autonomous role of Rb is insufficient to induce the severe and widespread apoptosis and differentiation defects typically observed in *Rb*$^{-/-}$ embryos. Thus, we conclude that while some of the phenotypes observed in *Rb*$^{-/-}$ embryos are mainly due to loss of *Rb* in extraembryonic lineages and others are due to loss of *Rb* in fetal tissues, the massive neural apoptosis and erythroid defects observed in *Rb*$^{-/-}$ embryos are due to a deficiency of Rb protein in both. These findings address the cell-autonomous versus non-cell-autonomous controversy of how Rb regulates neuronal apoptosis and erythroid differentiation by showing that extraembryonic and fetal signaling converge to control these processes (de Bruin et al. 2003; Wu et al. 2003; Clark et al. 2004; Spike et al. 2004).

Discussion

Since the inception of gene ablation techniques in mice two decades ago, a significant but likely underrepresented number of knockout mouse models have been found to suffer from extraembryonic defects (Han and Carter 2001; Sapin et al. 2001). Some of these genes encode chromatin remodeling activities that function in the regulation of embryonic patterning, cell migration, proliferation, and apoptosis. Other genes encode activities that have not been linked to specific processes. Unfortunately, genetic systems to study the mechanism of gene networks and function in extraembryonic lineages are lacking. Here we developed novel genetic and imaging tools that provide a uniquely powerful system to identify and dissect how *Rb* and other gene pathways interact in the placenta and in turn impact fetal development. Three-dimensional imaging of *Rb* mutant placentas revealed a global disruption in placenta architecture, characterized by an increase in trophoblast proliferation, a decrease in labyrinth and vascular spaces, and a disorganization of the labyrinth–spongiotrophoblast interface. Importantly, complementary morula–ES cell aggregation and *cre*-mediated gene ablation techniques demonstrate that the global disruption of the labyrinth architecture can be manifested by the specific ablation of *Rb* in TS cells. We conclude that the loss of *Rb* in TS cells is the defining event that causes lethality of *Rb*$^{-/-}$ embryos.

Previous work suggested that lethality of *Rb*$^{-/-}$ embryos is due to massive apoptosis and severe anemia in the fetus (Clarke et al. 1992; Jacks et al. 1992; Lee et al. 1992). More recent work raised the possibility that these fetal defects could be due to non-cell-autonomous roles of *Rb* originating in the placenta (Wu et al. 2003). The results presented here suggest that apoptosis and anemia are unlikely to be responsible for the lethality of *Rb*$^{-/-}$ embryos since placental deletion of *Rb* is sufficient to cause lethality without the associated massive apoptotic and erythroid phenotypes. Rather, we suggest that fetal lethality might simply be a result of general placental dysfunction. Thus, we conclude that some phenotypes observed in *Rb*$^{-/-}$ embryos, such as mid-gestation lethality, are primarily due to loss of *Rb* in extraembryonic lineages. Other phenotypes such as incomplete skeletal muscle differentiation, ectopic proliferation, and apoptosis in the PNS and lens are due to loss of *Rb* in fetal tissues. Yet other phenotypes such as neural apoptosis and erythroid defects are due to the convergence of cell-autonomous and nonautonomous roles of *Rb* in the fetus and placenta (de Bruin et al. 2003; Wu et al. 2003; Clark et al. 2004; Spike et al. 2004).

Rb is expressed in all extraembryonic lineages (Wu et al. 2003) yet its loss appears to impact only TS cells. The fact that ablation of *Rb* in TS cells, but not in differentiated trophoblast derivatives, disrupts placental development suggests that the critical function of *Rb* resides in a TS cell population prior to the commitment of labyrinth trophoblast and spongiotrophoblast cell fates. These results also begin to define the window of time during which Rb function becomes pivotal. Our genetic analyses suggest that *Rb* is critical for TS cell homeostasis by regulating two related cellular processes: proliferation and differentiation. Here we identified E2F3 among E2F family members as one of the key downstream effectors of Rb that aids in the maintenance of the TS cell population. The specific loss of *E2f3* in *Rb*$^{-/-}$ TS cells reduces the ectopic proliferation of trophoblasts and thus provides the necessary space for the branched trophoblast network to evolve. As a result, *Rb–E2f3* doubly deficient placentas can support fetal life beyond the time when *Rb*$^{-/-}$ fetuses typically die. The fact that these doubly deficient placentas cannot support life to term, however, suggests that loss of *E2f3* is unable to correct all defects in *Rb*$^{-/-}$ TS cells, including those that could arise from incomplete differentiation. Having identified the TS cell as a critical site of Rb action, we can now begin to unravel the biochemical interactions that are relevant to how Rb in this cell impacts the rest of the developing embryo.

Recent findings show a critical function of *Rb* in the maintenance of *Arabidopsis* root stem cells (Wildwater et al. 2005). Whereas ablation of Rb by RNAi or overexpression of E2F preserved and expanded stem cell populations in the columella and lateral root caps, overexpression of Rb or a cyclin-dependent kinase inhibitor led to depletion of this population. The role of Rb in this process appeared not to be related to the control of proliferation but rather in the maintenance of stem cell identity. Our results describing an effect of Rb in a murine extraembryonic stem cell niche extend these observations to higher eukaryotes. Moreover, we identified E2F3 as the critical Rb-binding partner involved in the

proliferative maintenance of this stem cell population. We propose that TS cells, unlike their lineage derivatives (labyrinth trophoblasts and spongiotrophoblasts), represent a compartment that is particularly susceptible to loss of *Rb*, possibly because p107 and p130 may not have the capacity to functionally compensate, even though these related proteins are clearly present in TS cells. The basis for the specificity in pocket protein function is not yet clear, but could involve the selective binding of Rb to E2F3. The properties that make Rb unique in TS cells may also be relevant in stem cells of other tissues. These observations raise the possibility that stem cell-specific functions of *Rb* described here may be related to its unique ability among pocket proteins to function as a tumor suppressor.

Materials and methods

Mouse strains and genotyping

$Rb^{+/-}$ (Jacks et al. 1992), $Rb^{LoxP/LoxP}$ (Marino et al. 2000), $Rosa^{LoxP}$ reporter (Soriano 1999), *CYP19-cre*, and *Tpbp-cre* (A.L. Fortier, H. Yamamoto, and J.C. Cross, in prep.) transgenic mice were maintained on a mixed background (C57BL/6 × 129/Sv × FVB/N). The $Rb^{\Delta 19}$ allele used in aggregation experiments was generated by in vivo knockout of the Rb^{LoxP} allele. PCR genotyping was used for mice, embryos, and placentas (primer sequences can be provided on request). DNA samples from transgenic *cre* lines were digested with BglII and hybridized with a DNA fragment encoding the *cre* ORF to probe Southern blots. Southern blot analysis of chimeric embryos generated by aggregation methods was carried out on EcoRV/NdeI-digested genomic DNA using a standard method.

Computational 3D imaging

$Rb^{+/+}$ and $Rb^{-/-}$ E13.5 embryos were collected from timed pregnancies, fixed in 10% buffered formalin, embedded in paraffin, serially sectioned at 5-µm intervals, and stained with hematoxylin and eosin (H&E). Stained sections from the entire placenta (~1200 sections; $n = 6$ placentas) were digitally scanned with an Aperio ScanScope using a 20× objective. Images were registered with rigid registration algorithms that employ a preprocessing *k*-means clustering step for foreground extraction and a principal component analysis (PCA) step for prealignment (Mosaliganti et al. 2006). The latter step is essential for expedient convergence of the underlying optimization procedure, an essential component of all registration algorithms (Maes et al. 1997). The registration algorithms of the NLM/NIHs' Insight Toolkit (ITK) (Ibanez 2003) were modified to align the two-dimensional (2D) sections. Simultaneously, each of the sections was segmented into tissue regions. Initial classification of cell types in the placenta was performed at the pixel level either by a Bayesian probability-based algorithm or the *k*-means clustering algorithm. Later, through the use of features such as cytoplasm/nuclear color, size, and density of nuclei and presence of vacuoles or RBCs, regions were classified into various tissue types by a Bayesian probability-based segmentation algorithm. Training of the segmentation algorithm was performed by a pathologist. The volumetric stack containing the segmented and mutually registered images was visualized using appropriate 3D volume-rendering algorithms (Sharp et al. 2007). The Volview application from Kitware, Inc., was used to create the final images. Ten individual sections from regular intervals throughout the placenta were used for human-validated segmentation of placental cell types and for morphometric measurement of tissue volumes (Sharp et al. 2007). Two different types of morphometirc analyses were used to evaluate the labyrinth–spongiotrophoblast interface. Contact surface areas were determined by Hausdorff dimension calculations. Spongiotrophoblast intrusions/extrusions were determined by evaluating each point in the labyrinth through the use of contour-tracking transfer functions (Mosaliganti et al. 2006) and numerical values were compiled from the entire placenta. Lower mean values indicate fewer finger-like projections, and lower standard deviations indicate a more uniform distribution of finger-like projections.

Tetraploid and diploid aggregations

Tetraploid aggregations were performed as described previously, with the exception that tetraploid and diploid embryos were aggregated at a 1:1 ratio (Wang et al. 1997; Wu et al. 2003). Aggregation of diploid embryos with YC5 ES cells was performed by methods similar to the tetraploid aggregations, except without the electrofusion step at E1.5. Genotyping of the resulting placentas was facilitated by the use of two different *Rb*-null alleles (Rb^{-} and $Rb^{\Delta 19}$) (Jacks et al. 1992; Marino et al. 2000). Fluorescent microscopy and Southern blot analysis demonstrated that the reconstituted chimeric fetuses had a high degree of contribution derived from $Rb^{+/+}$ YFP-positive YC5 ES cells (Hadjantonakis et al. 2002).

Histology and special stains

Embryos and placentas were collected from timed pregnancies, and whole-mount samples or 10-µm frozen sections from each embryo were stained with X-gal to monitor *cre* expression. Pregnant dams were injected with BrdU 1.5 h prior to harvest. Tissue from embryo aggregations was fixed in 10% buffered formalin, and tissue from transgenic crosses was either immediately fixed in 2% formaldehyde or frozen in OCT freezing medium and stored at –80°C. Proliferation was measured by immunostaining sections with BrdU-specific antibodies from DAKO (clone Bu20a), and apoptosis was detected by TUNEL assays using the Apoptag Plus Peroxidase In Situ Apoptosis Detection Kit (Chemicon International). Macrophages in fetal livers were detected using F4/80-specific antibodies (Caltag Laboratories, catalog no. MF48000) and quantified morphometrically by Matlab software. Frozen sections were used for in situ hybridization with antisense and sense RNA probes specific for the *Tpbp* gene. Blood smears were fixed in methanol and stained with Giemsa for quantification of nucleated RBCs.

Quantitative real-time RT–PCR

Placentas were collected from E13.5 embryos and homogenized to obtain single-cell suspensions that were used for total RNA isolation with TRIzol reagent (Life Technologies). Two micrograms to 10 µg of total RNA was used to generate cDNA using SuperScript III RT (Invitrogen). Real-time RT–PCR was performed using the Bio-Rad iCycler PCR machine. Each PCR reaction contained 2.0 µL of cDNA template, primers at a concentration of 100 nM, and 1× of SYBR Green Reaction Mix (Bio-Rad). Reactions were done in a final volume of 25 µL in triplicate, and data were analyzed using the ΔCt method, where *GAPDH* served as the internal control. Each PCR reaction gen-

erated only the expected amplicon as shown by the melting-temperature profiles of the final products, gel electrophoresis, and sequencing.

Acknowledgments

We thank A. Nagy for providing the YC5 ES cell line and K. Vintersten for assistance with embryo aggregations. We are grateful for technical assistance provided by J. Moffitt, J. Opavska, A. Gulacy, S. Kharzai, and Z. Barsman. We also thank M. Weinstein, A. Simcox, M. Ostrowski, and members of the Leone laboratory for critically reading the manuscript and helpful suggestions. This work was funded by NIH grants to G.L. (R01CA85619, R01CA82259, R01HD047470, P01CA097189), NIH grant to J.S. (BISTI P20 EB000591), NSF grants to J.S. (ANI-0330612, EIA-0203846, CNS-0615155, CNS-0509326, CNS-0426241), NSF grants to R.M. (0234273 and 0326386), NIH grant to L.W. (K01CA102328), and DoD award to A.d.B. (BC030892). G.L. is the recipient of The Pew Charitable Trust Scholar Award and the Leukemia and Lymphoma Society Scholar Award.

References

Calzonetti, T., Stevenson, L., and Rossant, J. 1995. A novel regulatory region is required for trophoblast-specific transcription in transgenic mice. *Dev. Biol.* **171:** 615–626.

Clark, A.J., Doyle, K.M., and Humbert, P.O. 2004. Cell-intrinsic requirement for pRb in erythropoiesis. *Blood* **104:** 1324–1326.

Clarke, A.R., Maandag, E.R., van Roon, M., van der Lugt, N.M., van der Valk, M., Hooper, M.L., Berns, A., and te Riele, H. 1992. Requirement for a functional Rb-1 gene in murine development. *Nature* **359:** 328–330.

Classon, M., Salama, S., Gorka, C., Mulloy, R., Braun, P., and Harlow, E. 2000. Combinatorial roles for pRB, p107, and p130 in E2F-mediated cell cycle control. *Proc. Natl. Acad. Sci.* **97:** 10820–10825.

Cobrinik, D., Lee, M.H., Hannon, G., Mulligan, G., Bronson, R.T., Dyson, N., Harlow, E., Beach, D., Weinberg, R.A., and Jacks, T. 1996. Shared role of the pRB-related p130 and p107 proteins in limb development. *Genes & Dev.* **10:** 1633–1644.

de Bruin, A., Wu, L., Saavedra, H.I., Wilson, P., Yang, Y., Rosol, T.J., Weinstein, M., Robinson, M.L., and Leone, G. 2003. *Rb* function in extraembryonic lineages suppresses apoptosis in the CNS of *Rb*-deficient mice. *Proc. Natl. Acad. Sci.* **100:** 6546–6551.

Ewen, M.E., Faha, B., Harlow, E., and Livingston, D.M. 1992. Interaction of p107 with cyclin A independent of complex formation with viral oncoproteins. *Science* **255:** 85–87.

Faha, B., Ewen, M.E., Tsai, L.H., and Livingston, D.M. 1992. Interaction between human cyclin A and adenovirus E1A-associated p107 protein. *Science* **255:** 87–90.

Hadjantonakis, A.K., Macmaster, S., and Nagy, A. 2002. Embryonic stem cells and mice expressing different GFP variants for multiple non-invasive reporter usage within a single animal. *BMC Biotechnol.* **2:** 11.

Han, V.K. and Carter, A.M. 2001. Control of growth and development of the feto-placental unit. *Curr. Opin. Pharmacol.* **6:** 632–640.

Hu, N., Gutsmann, A., Herbert, D.C., Bradley, A., Lee, W.H., and Lee, E.Y. 1994. Heterozygous Rb-1 Δ 20/+ mice are predisposed to tumors of the pituitary gland with a nearly complete penetrance. *Oncogene* **9:** 1021–1027.

Iavarone, A., King, E.R., Dai, X.M., Leone, G., Stanley, E.R., and Lasorella, A. 2004. Retinoblastoma promotes definitive erythropoiesis by repressing Id2 in fetal liver macrophages. *Nature* **432:** 1040–1045.

Ibanez, L. 2003. *The ITK software guide*. Kitware, Inc., Clifton Park, NY.

Jacks, T., Fazeli, A., Schmitt, E.M., Bronson, R.T., Goodell, M.A., and Weinberg, R.A. 1992. Effects of an Rb mutation in the mouse. *Nature* **359:** 295–300.

James, R.M., Klerkx, A.H., Keighren, M., Flockhart, J.H., and West, J.D. 1995. Restricted distribution of tetraploid cells in mouse tetraploid <=> diploid chimaeras. *Dev. Biol.* **167:** 213–226.

Kamat, A. 1999. A 500-bp region, approximately ≈40 kb upstream of the human *CYP19* (aromatase) gene, mediates placenta-specific expression in transgenic mice. *Proc. Natl. Acad. Sci.* **96:** 4575–4580.

Kamat, A., Smith, M.E., Shelton, J.M., Richardson, J.A., and Mendelson, C.R. 2005. Genomic regions that mediate placental cell-specific and developmental regulation of human *Cyp19* (aromatase) gene expression in transgenic mice. *Endocrinology* **146:** 2481–2488.

Lasorella, A., Noseda, M., Beyna, M., Yokota, Y., and Iavarone, A. 2000. Id2 is a retinoblastoma protein target and mediates signalling by Myc oncoproteins. *Nature* **407:** 592–598.

LeCouter, J.E., Kablar, B., Hardy, W.R., Ying, C., Megeney, L.A., May, L.L., and Rudnicki, M.A. 1998a. Strain-dependent myeloid hyperplasia, growth deficiency, and accelerated cell cycle in mice lacking the Rb-related p107 gene. *Mol. Cell. Biol.* **18:** 7455–7465.

LeCouter, J.E., Kablar, B., Whyte, P.F., Ying, C., and Rudnicki, M. 1998b. Strain-dependent embryonic lethality in mice lacking the retinoblastoma-related p130 gene. *Development* **125:** 4669–4679.

Lee, E.Y., Chang, C.Y., Hu, N., Wang, Y.C., Lai, C.C., Herrup, K., Lee, W.H., and Bradley, A. 1992. Mice deficient for Rb are nonviable and show defects in neurogenesis and haematopoiesis. *Nature* **359:** 288–294.

Lee, M.H., Williams, B.O., Mulligan, G., Mukai, S., Bronson, R.T., Dyson, N., Harlow, E., and Jacks, T. 1996. Targeted disruption of p107: Functional overlap between p107 and Rb. *Genes & Dev.* **10:** 1621–1632.

Lees, E., Faha, B., Dulic, V., Reed, S.I., and Harlow, E. 1992. Cyclin E/cdk2 and cyclin A/cdk2 kinases associate with p107 and E2F in a temporally distinct manner. *Genes & Dev.* **6:** 1874–1885.

Li, Y., Graham, C., Lacy, S., Duncan, A.M., and Whyte, P. 1993. The adenovirus E1A-associated 130-kD protein is encoded by a member of the retinoblastoma gene family and physically interacts with cyclins A and E. *Genes & Dev.* **7:** 2366–2377.

Lipinski, M.M. and Jacks, T. 1999. The retinoblastoma gene family in differentiation and development. *Oncogene* **18:** 7873–7882.

Lipinski, M.M., Macleod, K.F., Williams, B.O., Mullaney, T.L., Crowley, D., and Jacks, T. 2001. Cell-autonomous and non-cell-autonomous functions of the Rb tumor suppressor in developing central nervous system. *EMBO J.* **20:** 3402–3413.

Maandag, E.C., van der Valk, M., Vlaar, M., Feltkamp, C., O'Brien, J., van Roon, M., van der Lugt, N., Berns, A., and te Riele, H. 1994. Developmental rescue of an embryonic-lethal mutation in the retinoblastoma gene in chimeric mice. *EMBO J.* **13:** 4260–4268.

MacPherson, D., Sage, J., Crowley, D., Trumpp, A., Bronson, R.T., and Jacks, T. 2003. Conditional mutation of *Rb* causes cell cycle defects without apoptosis in the central nervous

system. *Mol. Cell. Biol.* **23:** 1044–1053.
Maes, F., Collignon, A., Vandermeulen, D., Marchal, G., and Suetens, P. 1997. Multimodality image registration by maximization of mutual information. *IEEE Trans. Med. Imaging* **16:** 187–198.
Marino, S., Vooijs, M., van Der Gulden, H., Jonkers, J., and Berns, A. 2000. Induction of medulloblastomas in p53-null mutant mice by somatic inactivation of Rb in the external granular layer cells of the cerebellum. *Genes & Dev.* **14:** 994–1004.
Morris, E.J. and Dyson, N.J. 2001. Retinoblastoma protein partners. *Adv. Cancer Res.* **82:** 1–54.
Mosaliganti, K., Pan, T., Sharp, R., Ridgway, R., Iyengar, S., Gulacy, A., Wenzel, P., de Bruin, A., Machiraju, R., Huang, K., et al. 2006. Registration and 3D visualization of large microscopy images. In *Medical imaging 2006: Image processing.* Proceedings of the SPIE, Vol. 6144 (eds. J.M. Reinhardt et al.), pp. 923–934.
Mulligan, G. and Jacks, T. 1998. The retinoblastoma gene family: Cousins with overlapping interests. *Trends Genet.* **14:** 223–229.
Robanus-Maandag, E., Dekker, M., van der Valk, M., Carrozza, M.L., Jeanny, J.C., Dannenberg, J.H., Berns, A., and te Riele, H. 1998. p107 is a suppressor of retinoblastoma development in pRb-deficient mice. *Genes & Dev.* **12:** 1599–1609.
Saavedra, H.I., Wu, L., de Bruin, A., Timmers, C., Rosol, T.J., Weinstein, M., Robinson, M.L., and Leone, G. 2002. Specificity of E2F1, E2F2 and E2F3 in mediating Rb function. *Cell Growth Differ.* **13:** 215–225.
Sapin, V., Blanchon, L., Serre, A.F., Lemery, D., Dastugue, B., and Ward, S.J. 2001. Use of transgenic mice model for understanding the placentation: Towards clinical applications in human obstetrical pathologies? *Transgenic Res.* **10:** 377–398.
Sharp, R., Ridgway, R., Mosaliganti, K., Wenzel, P., Pan, T., de Bruin, A., Machiraju, R., Huang, K., Leone, G., and Saltz, J. 2007. Volume rendering phenotype differences in microscopy data. *Journal of Computing in Science and Engineering* (in press).
Soriano, P. 1999. Generalized *lacZ* expression with the ROSA26 Cre reporter strain. *Nat. Genet.* **21:** 70–71.
Spike, B.T., Dirlam, A., Dibling, B.C., Marvin, J., Williams, B.O., Jacks, T., and Macleod, K.F. 2004. The Rb tumor suppressor is required for stress erythropoiesis. *EMBO J.* **23:** 4319–4329.
Symonds, H., Krall, L., Remington, L., Saenz-Robles, M., Lowe, S., Jacks, T., and Van Dyke, T. 1994. p53-dependent apoptosis suppresses tumor growth and progression in vivo. *Cell* **78:** 703–711.
Tanaka, S., Kunath, T., Hadjantonakis, A.K., Nagy, A., and Rossant, J. 1998. Promotion of trophoblast stem cell proliferation by FGF4. *Science* **282:** 2072–2075.
Trimarchi, J.M. and Lees, J.A. 2001. Sibling rivalry in the E2F family. *Mol. Cell. Biol.* **3:** 11–20.
Tsai, K.Y., Hu, Y., Macleod, K.F., Crowley, D., Yamasaki, L., and Jacks, T. 1998. Mutation of *E2f-1* suppresses apoptosis and inappropriate S phase entry and extends survival of *Rb*-deficient mouse embryos. *Mol. Cell* **2:** 293–304.
Uy, G.D., Downs, K.M., and Gardner, R.L. 2002. Inhibition of trophoblast stem cell potential in chorionic ectoderm coincides with occlusion of the ectoplacental cavity in the mouse. *Development* **129:** 3913–3924.
Vanderluit, J.L., Ferguson, K.L., Nikoletopoulou, V., Parker, M., Ruzhynsky, V., Alexson, T., McNamara, S.M., Park, D.S., Rudnicki, M., and Slack, R.S. 2004. p107 regulates neural precursor cells in the mammalian brain. *J. Cell Biol.* **166:** 853–863.
Wang, Z.Q., Kiefer, F., Urbanek, P., and Wagner, E.F. 1997. Generation of completely embryonic stem cell-derived mutant mice using tetraploid blastocyst injection. *Mech. Dev.* **62:** 137–145.
Weinberg, R.A. 1995. The molecular basis of oncogenes and tumor suppressor genes. *Ann. N. Y. Acad. Sci.* **758:** 331–338.
Wildwater, M., Campilho, A., Perez-Perez, J.M., Heidstra, R., Blilou, I., Korthout, H., Chatterjee, J., Mariconti, L., Gruissem, W., and Scheres, B. 2005. The RETINOBLASTOMA-RELATED gene regulates stem cell maintenance in Arabidopsis roots. *Cell* **123:** 1337–1349.
Williams, B.O., Schmitt, E.M., Remington, L., Bronson, R.T., Albert, D.M., Weinberg, R.A., and Jacks, T. 1994. Extensive contribution of Rb-deficient cells to adult chimeric mice with limited histopathological consequences. *EMBO J.* **13:** 4251–4259.
Wu, L., de Bruin, A., Saavedra, H.I., Starovic, M., Trimboli, A., Yang, Y., Opavska, J., Wilson, P., Thompson, J.C., Ostrowski, M.C., et al. 2003. Extra-embryonic function of Rb is essential for embryonic development and viability. *Nature* **421:** 942–947.
Yamasaki, L., Bronson, R., Williams, B.O., Dyson, N.J., Harlow, E., and Jacks, T. 1998. Loss of E2F-1 reduces tumorigenesis and extends the lifespan of $Rb1^{+/-}$ mice. *Nat. Genet.* **18:** 360–364.
Ziebold, U., Reza, T., Caron, A., and Lees, J.A. 2001. E2F3 contributes both to the inappropriate proliferation and to the apoptosis arising in *Rb* mutant embryos. *Genes & Dev.* **15:** 386–391.